



## Relationship between amplitude anisotropy and compressive strength of reinforced concrete depending on curing conditions

Nevbahar Ekin<sup>a\*</sup>

<sup>a</sup>Department of Geophysical Engineering, Suleyman Demirel University, Isparta 32260, Turkey

*Received: 27 Oct 2020; Accepted: 12 April 2021*

Determination of anisotropy has crucial to assess the quality of the concrete structures. The signal amplitudes of ultrasonic wave measured on different surfaces of concrete can be used for determining the anisotropy. In this study, a total of 27 cube reinforced concrete samples with different strengths (low, medium and high) have prepared. First, signals of ultrasonic waves (P and S waves) have obtained to use direct measurement technique from two opposite surfaces of the all samples. After, Fast Fourier Transform (FFT) has applied on ultrasonic signals for determining amplitude anisotropies and amplitude ratios. Finally, amplitude anisotropies and ratios have correlated with concrete strength, porosity and reinforcement diameter depending on curing conditions and new equations have developed. In addition, these equations have determined both depending on curing conditions and regardless of curing type. As a result, it has been shown that P and S wave amplitude anisotropies and ratios of reinforced concrete increased with decreasing of concrete strength. These increasing have obtained higher for P wave than that of S wave.

**Keywords:** Amplitude anisotropy, Amplitude ratio, Reinforced concrete, Ultrasonic waves, Porosity, Curing conditions

### 1 Introduction

All of reinforced concrete structures have exposed to natural hazards or dangerous loading conditions. The increase in intensity of loads such as earthquake, wind and change in environmental conditions has reduced the life cycle of reinforced concrete structures. Therefore, existing structures need to be monitored to ensure the health, integrity and safety of concrete aging situation regularly<sup>1-3</sup>. Generally, in civil engineering applications, the quality control of reinforced concrete structures has determined on the strength of core taken of certain points of the existing structures by Uniaxial Compressive Strength (UCS) test. However, same properties have not occurred throughout the concrete structure depending on the amount of fractures, cracks or pores. Accordingly, the determination of anisotropy has crucial for precise identification of concrete quality. Thus, the requirements of effective and reliable non-destructive testing methods have significantly increasing due to the rapid development of new materials and structures<sup>4,5</sup>.

In the context of this growing need in civil engineering, the non-destructive ultrasonic test method can respond to the industrial need<sup>6-8</sup>. The

destructive methods such as UCS test have simple and reliable but need to taking of core from structures. Therefore, destructive methods have not suitable for determining of strength due to need many cores in large scale reinforced concrete structures for not hazardous to the monumental tombs and historical structures. Another disadvantage of these methods has in sufficient evaluation of deterioration and damage of the structure as a function of time. The ultrasonic method can be used alone or in combination with various methods in order to evaluate the mechanical or environmental defects in concrete. In addition, this method has preferred due to its testing cost affordability, flexibility and ability to reveal the changes in microscopic size of the material<sup>9-22</sup>. With the ultrasonic method, even the presence of micro-cracks in a concrete material caused by the load on it over time or caused by the weakening of its strength can be detected. Because, since the transition time of the ultrasonic wave will be longer in any of the cracks, there has decreased in the ultrasonic velocity. Furthermore, non-destructive ultrasonic method has provided direct estimation of the mechanical and physical properties of the material such as strength, porosity, reinforcement state and aggregates etc.<sup>23</sup>. Ultrasonic method has allowed also practical and fast anytime

\*Corresponding author (E-mail: nevbaharsabbag@sdu.edu.tr)

repeated measurement<sup>24</sup>. However, in this method, interpretation of detected signals has become difficult due to multiple scattering, strong damping, mode conversion and nonlinear effects especially in solid and heterogeneous materials such as concrete<sup>7,25</sup>. Concrete, the most widely used building material, has obtained by mixing aggregate, water and chemical additives with cement which has a binding material<sup>4,25-28</sup>. Although this complexity causes the uneven distribution of ultrasonic waves in concrete<sup>29-31</sup>, the amplitudes determined by ultrasonic method can be used to accurately identify fractures and cracks as they have more sensitive to anisotropy than velocity<sup>32</sup>.

In this study, amplitude anisotropies of reinforced concretes have determined by ultrasonic method depending on concrete strength, reinforcement diameter, porosity and curing conditions.

## 2 Materials and Methods

### 2.1 Preparation of reinforced concrete designs

The studies were carried out on the 3 concrete designs. In the study, crushed stone aggregate and Portland composite cement were used. Air entraining agent and super plasticizer chemical additives were used in concrete mix. In order to determine the effect of curing conditions on anisotropy, 9 samples were subjected to water curing and the other 9 samples were subjected to air curing. In addition, 9 samples were used for determining porosity of concretes cured in oven. The water-cured samples were kept in the laboratory at a relative humidity of  $60 \pm 5\%$  in the cure pool at  $20 \pm 2^\circ\text{C}$  until the day of their measurements. The air-cured samples were kept in outside at the average temperature of  $20.3^\circ\text{C}$  and humidity of 48%.

In order to determine the porosity of the samples in the oven group, their densities were determined and ultrasonic seismic measurements were taken on them. Then, samples were dried in the oven at  $105^\circ\text{C}$  for 24 hours. After determining the dry and water-saturated weights of the samples taken from the oven, ultrasonic seismic measurements were taken again. One of the most important advantages of the ultrasonic method was that it allows repeated measurements to be taken in this way. The samples were placed in water pool for 28 days and were broken at the end of the 28<sup>th</sup> day with UCS test. A total of 27 samples were prepared as 9 cubic concrete samples for each design with  $150\text{ mm}^3$  size. Then, one

of the reinforcement (with a diameter of 10, 14 or 20 mm and a length of 250 mm) was placed in the center of these samples. For each design, one of reinforcement was placed in the middle of samples with a diameter of 10 mm in 3 samples, with a diameter of 14 mm in 3 samples and with a diameter of 20 mm in 3 samples.

### 2.2 Uniaxial compressive strength (UCS) test

In the UCS test, the concrete compressive strength was determined by applying hydraulic pressure on the concrete samples that between the steel plates in the device and breaking of samples<sup>33</sup>. While concrete compressive strength was obtained with Form + Test Alpha device, crushing was carried out with the reinforcement in the sample facing the side surface. The rate of load application on the samples was applied an average 13.5 kN/s ( $0.6 \pm 0.2\text{ MPa/s}$ ). In this study, the strengths of 3 samples in each design were determined with UCS test on the 28<sup>th</sup> day. Accordingly to this, the degree of anisotropy in reinforced concretes with different strength was determined by amplitude analysis. After then, the obtained results were compared with each other.

### 2.3 Ultrasonic method

The ultrasonic method was based on the principle of measuring the transit time of artificially generated high-frequency sound waves passed through concrete. Since the passing waves in the porous material through the concrete were slow, the voids or cracks in the concrete were the most important factors affecting the velocity. While higher of velocity indicated higher concrete quality, the low velocity indicated lower concrete quality<sup>34-36</sup>. The P waves were the waves that reach the source first, which could be propagated in any medium such as solid, liquid and gas. In addition, its particle motion was the same as the direction of wave propagation. The S waves were the waves that reach the source second and whose particle motion was perpendicular to the wave propagation direction. Since the rigidity was zero in liquid and gas, S waves were not affected by the pores in the concrete being liquid or gas. Because S waves propagated only in solids<sup>19</sup>. This was very important information in terms of interpreting the type of saturation of the pores. Porous materials with several micro cracks such as concretes and rocks, ultrasonic P wave was preferred for determining elastic properties in-situ and in most of the laboratory studies<sup>4,37-39</sup>. However, P wave velocity was more related to the solid part rather than

micro structural changes such as internal micro cracks and micro voids in concrete materials<sup>18,40</sup>. Therefore, only large cracks could be found by using P wave alone<sup>40</sup>. In recent years, S wave velocity was also required in dry and water saturated rocks and concretes for geotechnical evaluation of the ground or structures<sup>37</sup>. S wave velocity was depended on several features such as the strength of the concrete, properties of the cement, and aggregate type. In addition, fracture, void and alteration status of concrete could be determined and water saturation or dryness in concrete pores could be interpreted by using P and S wave velocities together<sup>36</sup>.

Ultrasonic elastic wave methods were constituted an important class of non-destructive evaluation techniques for concrete structures<sup>1,41</sup>. Comprehensive researches were conducted to determine the effect of cracks with ultrasonic waves<sup>42-48</sup>. In this study, the receiver and transmitter probes connected to the test equipment (OYO Sonic Viewer SXModel-5251C) were placed on two opposite sides of the reinforced concrete samples (surface AA' or BB' in Fig. 1) for obtaining P and S signals. The P and S pulses were sent to the sample with 200 and 100 kHz frequencies and travel times of the waves were measured. Three stacks were applied on the all of P and S wave measurements. In reinforced concrete structures surface cracks usually occurred. The development of such cracks in these structures facilitated the access of corrosive materials to the reinforcement and leading to an increased risk. Therefore, it was important to precisely identify and characterize these fractures, cracks and voids to evaluate and improve the structural reliability and durability of concrete structures<sup>41</sup>.

Changes in ultrasonic wave velocities depended on magnitude, measurement direction (relative to the direction of wave propagation), conditions (such as

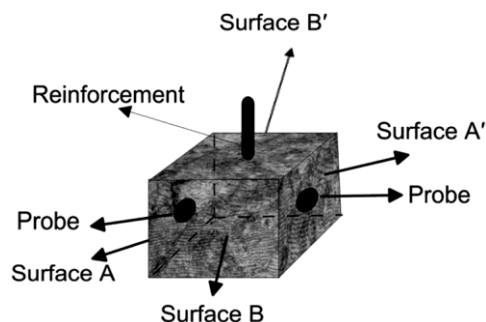


Fig. 1 — Measurement direction in concrete surfaces using direct measure technique with ultrasonic device.

void or filler) and volumetric crack distribution<sup>4</sup>. Researchers attempting to reveal the anisotropic structure of reinforced concrete were generally utilized ultrasonic pulse velocity measurements at various materials<sup>1</sup>. Directional dependence of ultrasonic wave velocities was made by some researchers for metals<sup>49</sup> or rocks<sup>50</sup>. Shokouhi *et al.*<sup>4</sup> tried to determine the anisotropy by using surface waves in the sonic frequency range with acoustic emission technique on concrete. However, in this study anisotropy degree of concrete was determined by using nondestructive P and S wave signals by taking care of curing conditions, different strength of concretes, reinforcement diameter and age of concrete.

### 2.3.1 Fast Fourier Transform (FFT)

FFT was used in geophysics and many other sciences to convert sampled signals from time domain to frequency domain. In other words, it was the separation of any signal into frequency, amplitude and phase information as geophysical signals were generally defined in time and space domain<sup>51,52</sup>. In order to analyze the data, it was very important to move it to the frequency/wave number domain. The data obtained by transferring the data observed in time domain to the frequency domain was called spectrum. FFT was used to indicate the change of magnitudes such as energy or amplitude in the time domain according to parameters such as frequency or wave number in the frequency domain<sup>53</sup>. A periodic signal could be expressed as the sum of many sine and cosine signals of various amplitude and frequency. The frequency content of seismic waves varied with time. In order to better understand the structure of seismic signals, examining the change of signals over time, along with the frequency content of the signal was crucial. However, it was not clear what time intervals coincide to the amplitudes of the signal in the frequency domain. Mathematically, FFT of a  $f(t)$  signal was given with  $F(\omega)$  in Eqs (1-3) (where  $\omega$  was referred to the angular frequency):

$$f(t) \xrightarrow{FFT} F(\omega) \quad \dots (1)$$

$$f(t) = \frac{1}{\sqrt{2\pi}} \int_{-\infty}^{\infty} F(\omega) e^{-i\omega t} d\omega \quad \dots (2)$$

$$F(\omega) = \frac{1}{\sqrt{2\pi}} \int_{-\infty}^{\infty} f(t) e^{i\omega t} dt \quad \dots (3)$$

The FFT was defined in terms of real-imaginary components in Eq. (4).

$$F(\omega) = a(\omega) - ib(\omega) \quad \dots (4)$$

The FFT was defined in terms of amplitude and phase spectrum in Eq. (5).

$$F(\omega) = |F(\omega)|e^{i\phi(\omega)} \quad \dots (5)$$

Here, the amplitude spectrum and the phase spectrum could be defined in Eqs (6-7), respectively.

$$|F(\omega)| = [a^2(\omega) - b^2(\omega)]^{1/2} \quad \dots (6)$$

$$\phi(\omega) = \tan^{-1} \frac{-b(\omega)}{a(\omega)} + 2n\pi \quad n = 0, \bar{1}, \bar{2}, \quad \dots (7)$$

The amplitude spectrum obtained by FFT shows the frequency content of the components of the analyzed wave and which component of the wave was large amplitude. The frequency corresponding to the greatest amplitude was defined as the dominant frequency of the examined wave and it was unique in every signal. Thus, the difference between the greatest amplitudes in dominant frequencies could help determine anisotropy. The high changes obtained from the ultrasonic wave measurements taken on reinforced concrete might indicate the anisotropy which might be caused by fractures, micro cracks, pores, irregular distribution of aggregate or the great number of reinforcement. Therefore, two P and two S wave travel time measurements were made from the opposing surfaces of the samples with ultrasonic method. Then, P and S wave signals obtained in the time domain were transferred to the frequency domain by means of FFT. The amplitude values corresponding to the dominant frequencies were determined for the same sample. One of these values was correspond to  $A_{max}$  and the other was  $A_{min}$ . With the help of these amplitudes, the degree of anisotropy was determined depending on the concrete strength and curing conditions.

**2.3.2 Amplitude anisotropy and amplitude ratio**

While isotropy was defined as the situation where the measurements taken at any point of the mass of the material present the same physical and mechanical properties in all directions<sup>54</sup>, anisotropy was defined as the change of these physical properties depending on direction<sup>55</sup>. Anisotropy differs from the rock feature called heterogeneity in one direction, whereas heterogeneity was the change between two or more points. Anisotropy in a concrete element caused changes in the ultrasonic velocity. Seismic anisotropy was related to the structure and texture of the material. Therefore, the analysis of seismic anisotropy provides important information for environmental and engineering applications as well as determining

reservoir properties<sup>56</sup>. The ultrasonic pulse velocity method was suitable for the relative evaluation of concrete homogeneity and therefore concrete quality<sup>57</sup>. Anisotropy of the medium in a crack-containing region could be estimated from ultrasonic measurements parallel to and perpendicular to the crack<sup>41</sup>. Some researchers were conducted research in various structures to determine the homogeneity of concrete<sup>34,58-60</sup>. Factors such as concrete type and compressive strength, tension, temperature, humidity, degradation (micro crack) were known to be effective on ultrasonic velocities and amplitudes<sup>28</sup>.

In fact, concrete was neither homogeneous nor completely linear elastic. In addition, ultrasonic waves were exposed to reflections or scattering within the internal boundaries of objects such as small cracks or reinforcement. In the damaged concrete due to cracks and similar defects, the frequency range of pulse was much higher than in undamaged concrete. Frequency analysis was used for a long time in ultrasonic testing of metals, but in concrete, this method was only recently applied<sup>61</sup>. The process of determining frequency modulation generally was required the conversion of the received waveform. This was done often with the Fourier transform<sup>62</sup>, but a very large set of data was required to provide good resolution with this transform. Processing of signals over time means that a number of frequencies were mixed in the analysis of signal amplitudes, but the transfer function of the power converter when considering the fairly narrow band; it was believed to be an acceptable processing area<sup>41</sup>. The degrees of anisotropy at seismic velocities were shown by Thomsen in Eqs (8 and 9)<sup>63</sup>. Here,  $\epsilon_v$  represents P wave velocity anisotropy and  $\gamma_v$  indicates S wave velocity anisotropy.

$$\epsilon_v = \frac{V_{pmax}^2 - V_{pmin}^2}{2V_{pmin}^2} \quad \dots (8)$$

$$\gamma_v = \frac{V_{smax}^2 - V_{smin}^2}{2V_{smin}^2} \quad \dots (9)$$

The degree of amplitudes anisotropy for the P and S wave could be obtained with Eq (10 and 11) by using Equations 8-9 (A was referred to amplitude parameter).

$$\epsilon_A = \frac{A_{pmax}^2 - A_{pmin}^2}{2A_{pmin}^2} \quad \dots (10)$$

$$\gamma_A = \frac{A_{smax}^2 - A_{smin}^2}{2A_{smin}^2} \quad \dots (11)$$

In this study, maximum values were obtained from AA' surface and minimum values were obtained from BB' surface of reinforced concretes. AA' signals (indicated by the blue line) were represented the maximum amplitudes, while B-B' signals (indicated by the green line) were represented the minimum amplitudes in the formulas given in Eqs (8-11). Amplitude anisotropy was determined from differences of the signal amplitudes in dominant frequencies. In addition, the amplitude ratios of P ( $G_P$ ) and S ( $G_S$ ) waves could be found by proportioning the amplitudes obtained from the signals measured on AA' and BB' surfaces. These were given in Eqs (12-13), respectively. While the amplitude ratio of value 1 indicates isotropy, moving away from value 1 might indicate that anisotropy was increased.

$$G_P = \frac{A_{Pmax} (AA')}{A_{Pmin} (BB')} \quad \dots (12)$$

$$G_S = \frac{A_{Smax} (AA')}{A_{Smin} (BB')} \quad \dots (13)$$

The amplitude anisotropies and ratios of P and S wave were advantages because the dominant frequencies in signals was constant and the amplitude values corresponding to these frequencies was also constant in this method.

### 3 Results and Discussion

#### 3.1 The signals and FFT responses of P and S waves

In this study, FFT method was applied on the P and S wave signals obtained from the two opposite surfaces of the reinforced concrete samples with different strengths and cured in water and air. FFT method was applied on all of P and S wave signals obtained from samples surfaces. Although, all of obtained results were used in interpretation, some selected figures were located in article. The P and S wave signals and FFT responses of several reinforced concretes with low, medium and high strength saturated in water or air cure were given in Figs 2 and 3, respectively.

Maximum amplitudes in FFT were corresponded to the values in dominant frequencies (red line) obtained from ultrasonic measurement on the AA' (blue line) and BB' (green line) surface of samples. According to these figures, when the FFT results of the signals obtained from two different surfaces of the same concrete sample were examined, it was seen that different maximum amplitude values were obtained at the same dominant frequency value (e.g. S wave signals in water cure), as well as different maximum

amplitude values at different dominant frequency values.

P and S wave amplitude values obtained from AA' and BB' surface of reinforced concretes with low, medium and high strength were presented in Table 1 depending on curing conditions and strength type. According to this, amplitude values obtained from measurements on AA' and BB' surfaces were represented the maximum and minimum amplitude values in Eqs (10-11). While, P wave amplitude values changed between 204-1308 dB in water cure, these were changed between 264-1504 dB in air cure. Similarly, while S wave amplitude values changed between 410-1573 dB in water cure, these were changed between 345-1555 dB in air cure. When Table was examined, it was observed that the greatest amplitude values in dominant frequencies were very different from each other. This change was expected to be very low in a homogeneous and isotropic material. According to the data obtained with this study, it caused different amplitude values to be obtained at the same or different dominant frequencies depending on the pore amount and the orientation direction of the pores in reinforced concrete of different strengths. This situation was also observed in Fig. 4 for water and air cured reinforced concrete samples. While S wave amplitude values obtained from measurements on AA' and BB' surfaces were shown in this figure with dashed and solid blue lines, these values of the P wave were shown with dashed and solid black lines, respectively.

#### 3.2 Relationships among amplitude ratios, amplitude anisotropies and reinforcement diameter depending on UCS and curing conditions

In terms of interpretation of anisotropy in concrete, amplitude values alone might not be meaningful. However, the presence and degree of anisotropy in concretes with different strengths could be revealed by calculating the amplitude ratio and amplitude anisotropy. Values of amplitude ratios of P ( $G_P$ ) and S ( $G_S$ ) waves and amplitude anisotropies of P ( $\epsilon_A$ ) and S ( $\gamma_A$ ) waves depending on reinforcement diameter (10, 14 or 20 mm) were given in Tables 2-3, respectively.

The change of amplitude ratios and anisotropies with reinforcement diameter depending on strength of concrete in water and air curing were given in Figs 5-6. In these figures, low, medium and high strength concretes were showed with solid blue, red and black lines, respectively. Since S waves were less

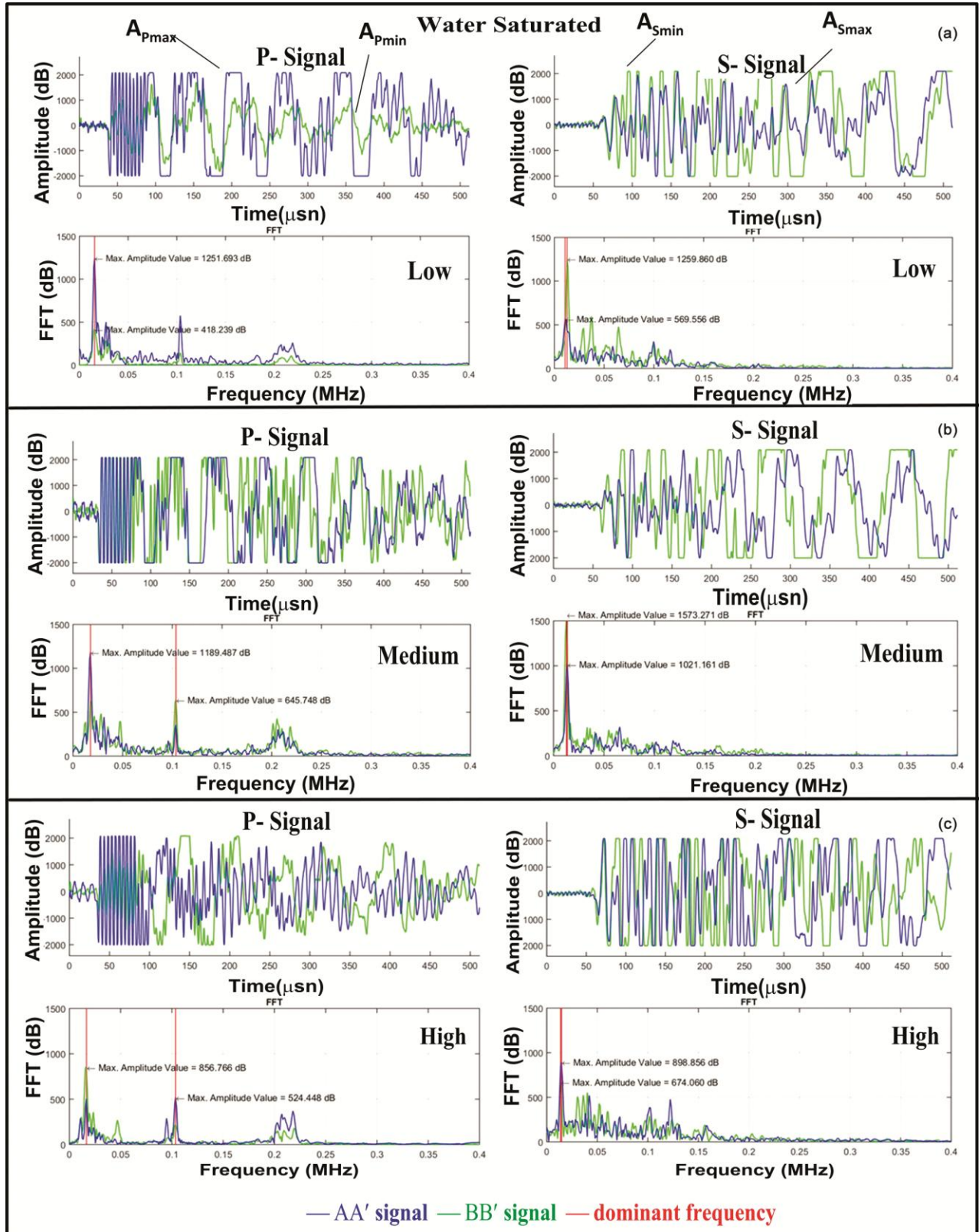


Fig. 2 — Signals and FFT responses of P and S waves of water saturated reinforced concretes with different (a) low, (b) medium, and (c) high strength.

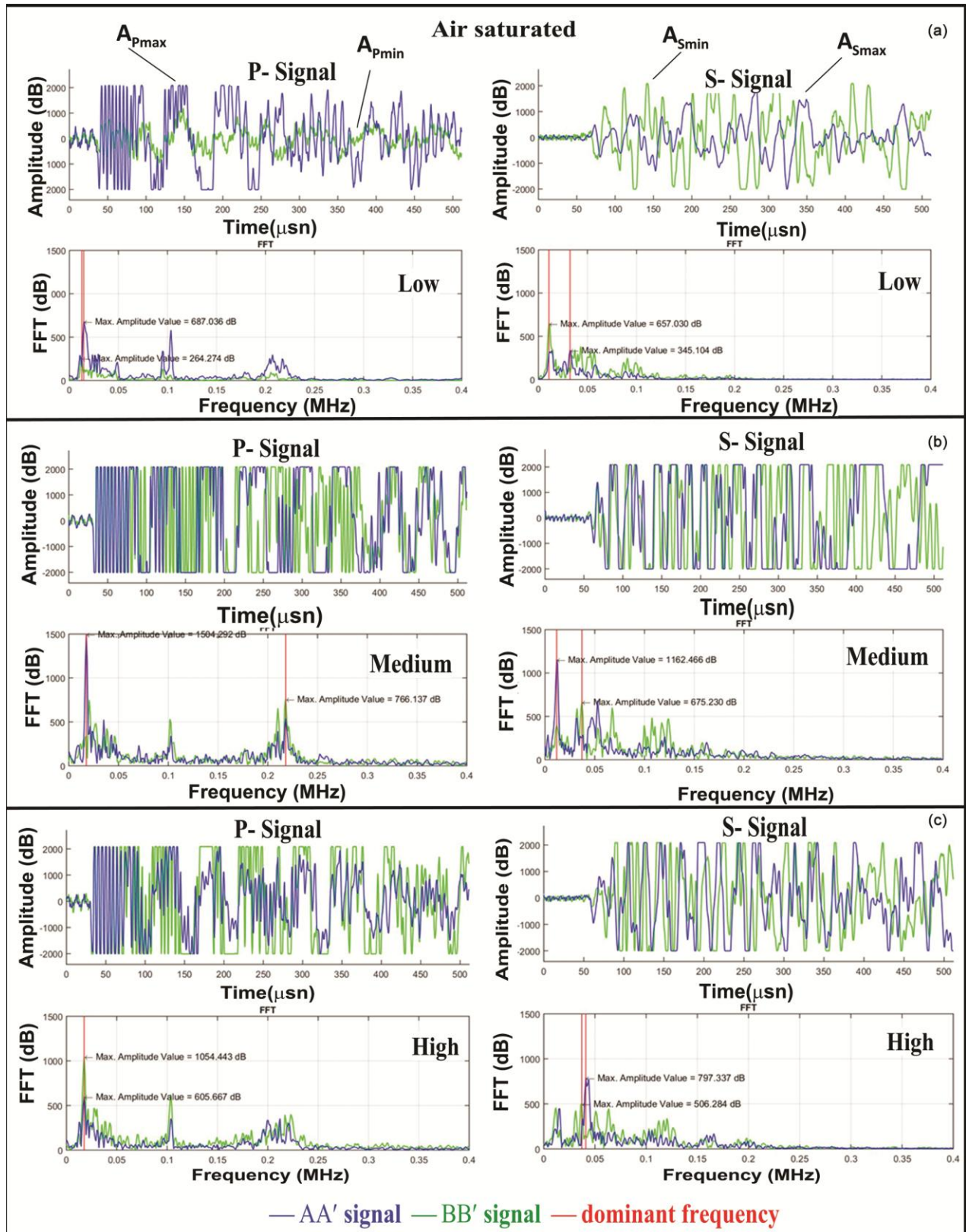


Fig. 3 — Signals and FFT responses of P and S waves of air saturated reinforced concretes with different (a) low, (b) medium, and (c) high strength.

affected by the saturation of the pores, the amplitude ratios and anisotropies were closer to each other in water and air curing. At the same time, amplitude ratios and anisotropies were obtained higher in low strength concretes. Furthermore, it could be seen from these figures that concrete strength types as well as curing conditions were also effective in amplitude

ratio and anisotropy. According to these figures, amplitude ratio and anisotropy were increased with increasing of reinforcement diameter. However, it would not be entirely correct to say that this effect was only due to the reinforcement effect. It was thought that this effect was caused not only by the diameter of the reinforcement but also from the

Table 1 — P and S wave amplitudes obtained from AA' and BB' surface of reinforced concretes

Cure type	UCS (MPa)	A <sub>P</sub> (AA') (dB)	A <sub>P</sub> (BB') (dB)	A <sub>S</sub> (AA') (dB)	A <sub>S</sub> (BB') (dB)
Water saturated concretes	4.8	1251.7	418.2	1259.9	569.6
	8.6	767.9	221.2	1097.0	410.9
	18.5	894.8	248.5	1480.1	542.1
	35.9	1189.5	645.7	1573.3	1021.2
	43.6	957.3	455.5	1408.1	870.0
	54.4	1308.9	480.9	1436.0	714.3
	55.7	856.8	524.4	898.9	674.1
	60.4	359.9	204.6	672.9	479.1
Air saturated concretes	61.6	997.2	550.4	1078.3	739.3
	4.7	687.0	264.3	657.0	345.1
	7.4	826.2	304.3	1357.7	640.7
	17.5	796.2	282.2	1060.7	479.8
	32.1	1341.8	737.7	1162.5	675.2
	41.1	1504.3	766.1	776.2	435.2
	53.7	1251.8	628.2	1555.8	858.9
	54.9	589.2	356.9	554.0	376.0
57.3	626.3	374.1	797.3	506.3	
60.9	1054.4	605.7	796.5	502.4	

Table 2 — Amplitude ratios obtained from P and S wave signals in water and air curing samples

Reinforcement diameter (ϕ) (mm)	Water saturated concretes			Air saturated concretes		
	UCS (MPa)	G(P <sub>sat</sub> )	G(S <sub>sat</sub> )	UCS (MPa)	G(P <sub>air</sub> )	G(S <sub>air</sub> )
10	18.5	3.6	2.2	17.5	2.6	1.9
10	54.4	1.8	1.5	53.7	1.8	1.7
10	61.6	1.6	1.3	60.9	1.7	1.5
14	8.6	3.5	2.7	7.4	2.7	2.1
14	43.6	2.1	1.6	41.1	2.0	1.8
14	60.4	1.8	1.4	57.3	1.7	1.6
20	4.8	3.0	2.7	4.7	2.8	2.2
20	35.9	2.7	2.0	32.1	2.0	1.8
20	55.7	1.8	1.5	54.9	1.7	1.6

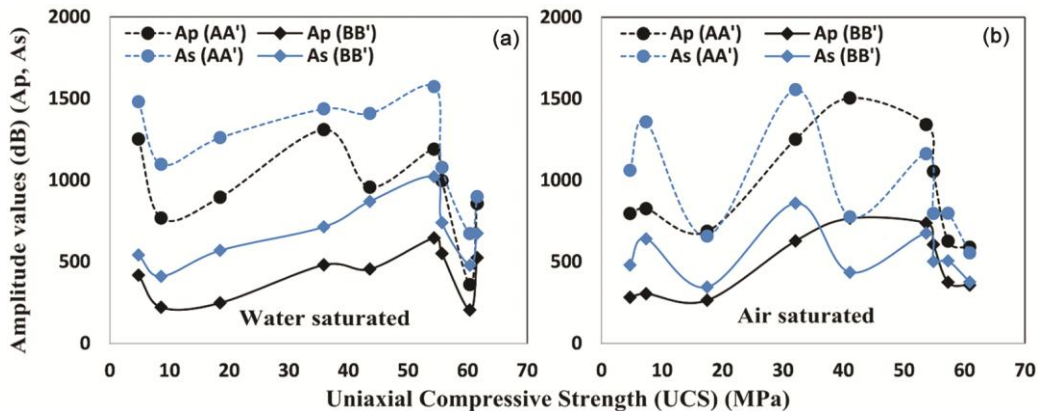


Fig. 4 — Comparison of UCS and amplitude values (AA' and BB') obtained from P and S wave signals for (a) water, and (b) air curing samples.

Table 3 — Amplitude anisotropy of reinforced concretes depending on reinforcement diameter

Reinforcement diameter ( $\phi$ ) (mm)	Water saturated concretes			Air saturated concretes		
	UCS (MPa)	$\epsilon_A(P_{sat})$	$\gamma_A(S_{sat})$	UCS (MPa)	$\epsilon_A(P_{air})$	$\gamma_A(S_{air})$
10	18.5	3.98	1.95	17.5	2.88	1.31
10	54.4	1.20	0.69	53.7	1.15	0.98
10	61.6	0.83	0.39	60.9	0.86	0.59
14	8.6	5.53	3.06	7.4	3.19	1.75
14	43.6	1.71	0.81	41.1	1.43	1.09
14	60.4	1.05	0.49	57.3	0.90	0.74
20	4.8	5.98	3.23	4.7	3.48	1.94
20	35.9	3.20	1.52	32.1	1.48	1.14
20	55.7	1.14	0.56	54.9	1.02	0.76

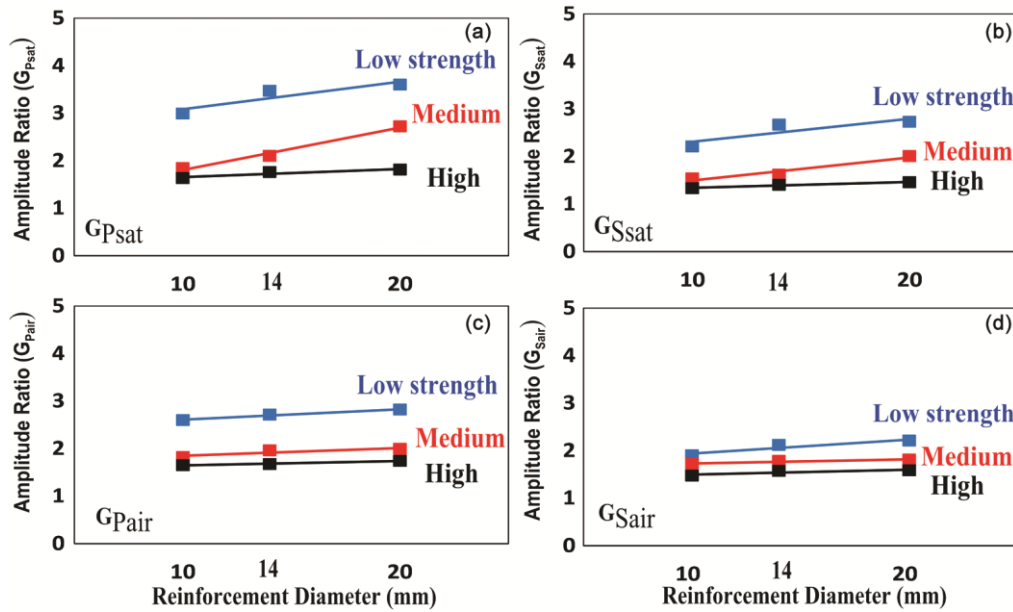


Fig. 5 — Variation of amplitude ratios with reinforcement diameter depending on concrete strength for water saturated samples ((a) P wave, and (b) S wave) and for air saturated samples ((c) P wave, and (d) S wave).

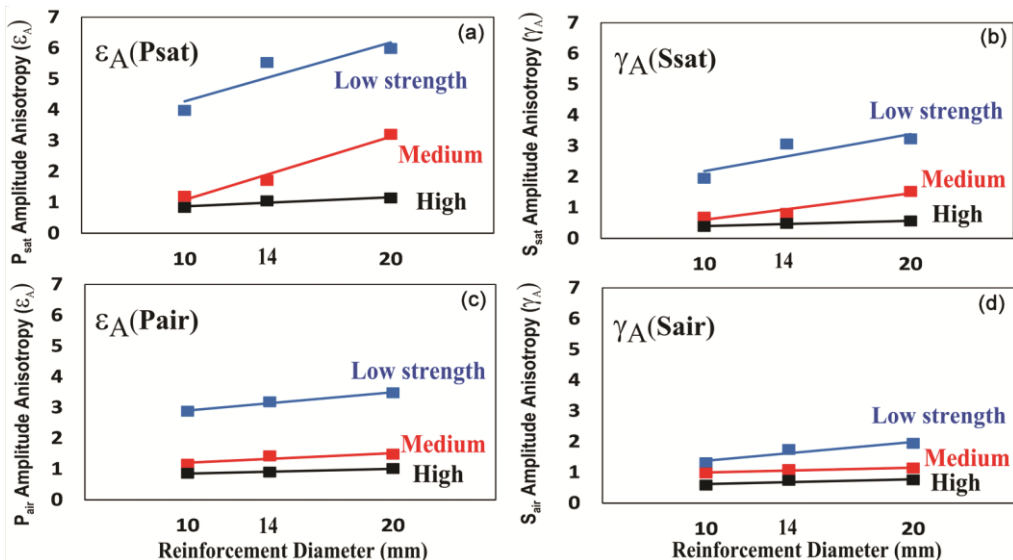


Fig. 6 — Variation of amplitude anisotropies with reinforcement diameter depending on concrete strength for water saturated samples ((a) P wave, and (b) S wave) and for air saturated samples ((c) P wave, and (d) S wave).

different porous structure of the samples depending on the concrete strength.

**3.3 Relationships among amplitude ratios, amplitude anisotropies, porosity and UCS depending on curing conditions**

Concrete strength and porosity values of water and air saturated reinforced concretes were given in Table 4. Porosity values given in Table were determined with using oven cured concrete samples.

According to this, concrete strength values varied between 4.80 MPa and 61.60 MPa for concretes cured in water. Similarly, these varied between 4.7 MPa and 60.9 MPa for concretes cured in air. In addition,

Table 4 — Concrete strength and porosity values of water and air saturated reinforced concretes

Uniaxial compressive strength (UCS) (MPa)		Porosity (n%)
Water saturated concretes	Air saturated concretes	
4.8	4.7	11.62
8.6	7.4	10.74
18.5	17.5	8.48
35.9	32.1	5.72
43.6	41.1	4.03
54.4	53.7	3.74
55.7	54.9	3.36
60.4	57.3	3.03
61.6	60.9	2.29

porosity values varied between 2.29% and 11.62%. It was seen that the porosity decreased with increasing of concrete strength.

Relationships between UCS, porosity, amplitude ratios and anisotropies were presented in Figs 7 and 8 depending on curing conditions (water or air saturated). These variations were shown with blue, green, red and purple lines for water cured ( $P_{sat}$ ,  $S_{sat}$ ) and for air cured ( $P_{air}$ ,  $S_{air}$ ) reinforced concrete samples, respectively. The reference line of anisotropy at value 1 was shown in red in these figures by a dashed line. Accordingly, P and S wave amplitude ratios were obtained higher in low strength concrete saturated in both water and air cure. While, in the low strength concrete P wave amplitude ratio varied between 3.0-3.6 in water concrete, it varied between 2.6-2.8 in air cure. Similarly, S wave amplitude ratio varied between 2.2-2.7 in water cure, it varied between 1.9 and 2.2 for low strength concrete cured in air. While, in the medium strength concrete P wave amplitude ratio varied between 2.1 and 2.7 values in water cure, it was approximately 2.0 in air cure. Similarly, S wave amplitude ratio was between 1.6-2.0 in water concrete, it was 1.8 in medium strength concrete cured in air. In the high strength concrete P wave amplitude ratio was generally

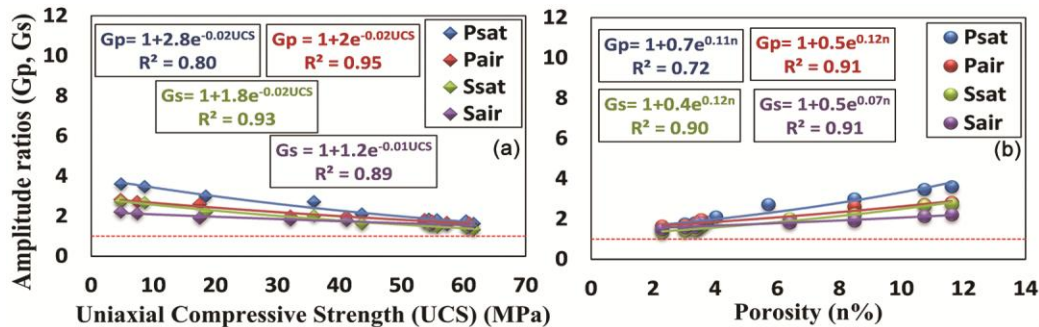


Fig. 7 — Relationships between (a) amplitude ratios and UCS, and (b) amplitude ratios and porosity, depending on curing conditions.

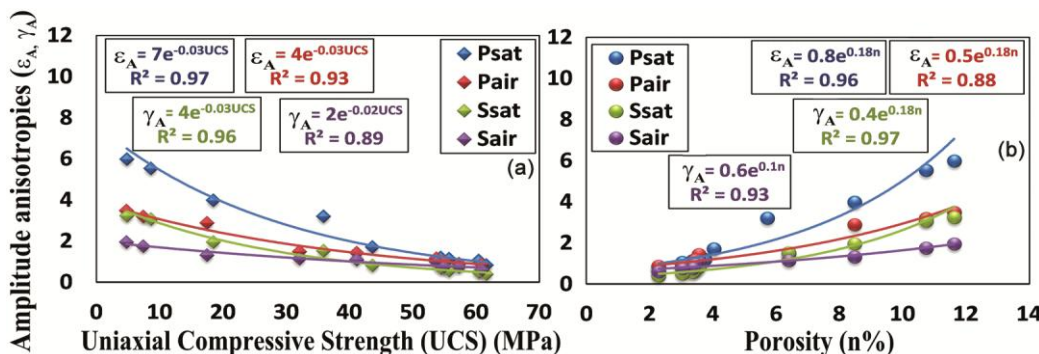


Fig. 8 — Relationships between (a) amplitude anisotropies and UCS, and (b) amplitude anisotropies and porosity, depending on curing conditions.

1.8 in water concrete and 1.7 in air cure. For high strength concrete cured in air, S wave amplitude ratio varied between 1.3-1.5 in water cure, it varied between 1.5-1.7 in air cured for high strength concrete.

Amplitude ratio of P wave and S wave could be calculated depending on the UCS for concrete samples in Eqs (14-15) for water curing samples and Eqs (16-17) for samples in air curing, respectively. Accordingly, the amplitude ratios decreased exponentially with the increase in concrete strength.

$$G(P_{sat}) = 1 + 2.8e^{-0.02UCS} \quad R^2=0.80 \quad \dots (14)$$

$$G(S_{sat}) = 1 + 1.8e^{-0.02UCS} \quad R^2=0.93 \quad \dots (15)$$

$$G(P_{air}) = 1 + 2.0e^{-0.02UCS} \quad R^2=0.95 \quad \dots (16)$$

$$G(S_{air}) = 1 + 1.2e^{-0.01UCS} \quad R^2=0.89 \quad \dots (17)$$

In addition, relationships between porosity and amplitude ratios of P and S wave of water and air saturated concrete samples were given in Eqs (18-21), respectively. Accordingly, amplitude ratios were increased with increasing of porosity of concrete. In addition, amplitude ratios of P and S wave of water cured concretes were higher than that of air cured concretes.

$$G(P_{sat}) = 1 + 0.7e^{0.11n} \quad R^2=0.72 \quad \dots (18)$$

$$G(S_{sat}) = 1 + 0.5e^{0.12n} \quad R^2=0.91 \quad \dots (19)$$

$$G(P_{air}) = 1 + 0.4e^{0.12n} \quad R^2=0.90 \quad \dots (20)$$

$$G(S_{air}) = 1 + 0.5e^{0.07n} \quad R^2=0.91 \quad \dots (21)$$

According to these new equations, the value 1 of amplitude ratio referred to isotropy, while moving away from value 1 referred to anisotropy. As could be seen from figure, while this ratio was higher in low strength concretes, it approached value 1 in high strength concretes. In addition, amplitude ratios were found to be higher for water cured low strength concretes compared to these in air cured. However, these ratios were found to be higher for high strength concretes in air cured than that of water cured concretes. The correlation coefficient  $R^2$  of the Equations was found in the range of 0.80-0.95 values.

In these figure samplitude anisotropies were calculated with the help of Eqs (10-11). While, in the low strength concrete P wave amplitude anisotropies varied between 3.98 and 5.98 in water concrete, it varied between 2.88 and 3.48 in air cure. Similarly, S wave amplitude anisotropy varied between 1.95 and 3.23 in water cure, it varied between 1.31-1.94 for

low strength concrete cured in air. While, in the medium strength concrete P wave amplitude anisotropy varied between 1.20 and 1.71 in water cure, it varied between 1.15 and 1.43 in air cure. Similarly, S wave amplitude anisotropy varied between 0.69 and 0.81 in water concrete, it varied between 0.98-1.09 in air cured for medium strength concrete. In the high strength concrete P wave amplitude anisotropy varied between 0.83-3.20 in water cure, it varied between 0.86-1.48 in air cure. Similarly, S wave amplitude anisotropy varied between 0.39-1.52 in water cure, it varied between 0.59-1.14 in air cured for high strength concrete.

With this study, new Eqs (22-25) were developed for estimation of P or S wave amplitude anisotropy from UCS depending on curing conditions.

$$\varepsilon_A(P_{sat}) = 7e^{-0.03UCS} \quad R^2=0.97 \quad \dots (22)$$

$$\varepsilon_A(P_{air}) = 4e^{-0.03UCS} \quad R^2=0.93 \quad \dots (23)$$

$$\gamma_A(S_{sat}) = 4e^{-0.03UCS} \quad R^2=0.96 \quad \dots (24)$$

$$\gamma_A(S_{air}) = 2e^{-0.02UCS} \quad R^2=0.89 \quad \dots (25)$$

In addition, new Eqs (26-29) were defined for determination of these anisotropies from porosity depending on curing conditions.

$$\varepsilon_A(P_{sat}) = 0.8e^{0.18n} \quad R^2=0.96 \quad \dots (26)$$

$$\varepsilon_A(P_{air}) = 0.5e^{0.18n} \quad R^2=0.88 \quad \dots (27)$$

$$\gamma_A(S_{sat}) = 0.4e^{0.18n} \quad R^2=0.97 \quad \dots (28)$$

$$\gamma_A(S_{air}) = 0.6e^{0.10n} \quad R^2=0.93 \quad \dots (29)$$

While P and S wave amplitude anisotropies decreased with increasing of UCS of concrete, they increased with increasing of porosity of concrete. In addition, amplitude anisotropy decreased the most in the  $\varepsilon_A(P_{sat})$  and it decreased the least in the  $\gamma_A(S_{air})$ . This situation could be explained as S wave was less affected by saturation.

The relationships between concrete strength, porosity, amplitude ratios and anisotropies were presented in Figs 9 and 10, regardless of curing conditions. Amplitude ratios and anisotropies of P wave and S wave were shown with black and blue lines, respectively. With the help of these equations, P or S wave amplitude ratios and anisotropies depending on concrete strength or porosity could be predicted for all concrete types regardless of curing conditions.

According to this, P and S amplitude ratios could be calculated from the Eqs (30-33) by using concrete strength or porosity regardless of curing conditions.

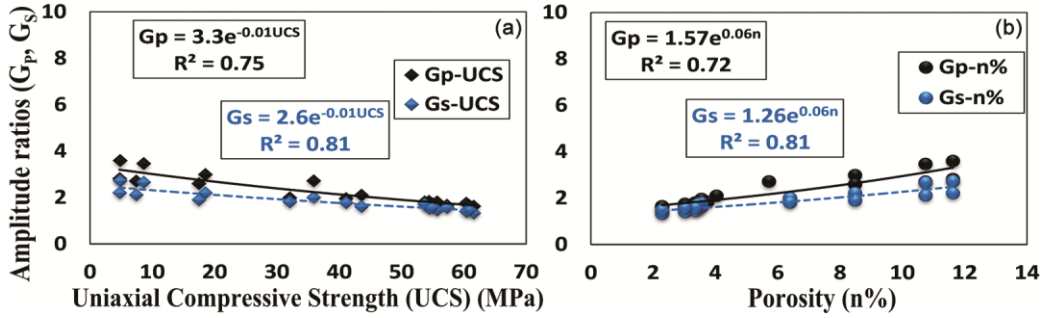


Fig. 9 — Relationships between (a) amplitude ratios and UCS, and (b) amplitude ratios and porosity, regardless of curing conditions.

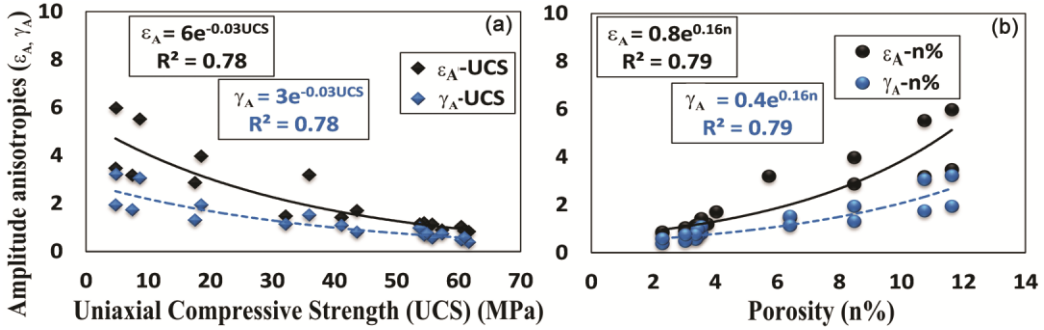


Fig. 10 — Relationships between (a) amplitude anisotropies and UCS, and (b) amplitude anisotropies and porosity, regardless of curing conditions.

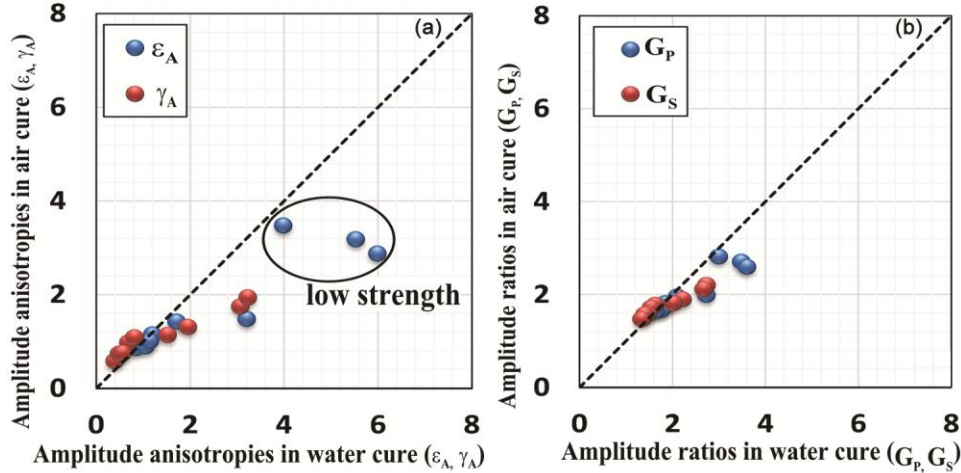


Fig. 11 — Comparison of (a) amplitude anisotropies of P and S waves, and (b) amplitude ratios of P and S waves, depending on the cure conditions.

$$G_p = 3.3e^{-0.01UCS} \quad R^2=0.75 \quad \dots (30)$$

$$G_s = 2.6e^{-0.01UCS} \quad R^2=0.81 \quad \dots (31)$$

$$G_p = 1.57e^{0.06n} \quad R^2=0.72 \quad \dots (32)$$

$$G_s = 1.26e^{0.06n} \quad R^2=0.81 \quad \dots (33)$$

In addition, P and S amplitude anisotropy could be calculated from the Eqs (34-37) by using concrete strength or porosity regardless of curing conditions.

$$\epsilon_A = 6e^{-0.03UCS} \quad R^2=0.78 \quad \dots (34)$$

$$\gamma_A = 3e^{-0.03UCS} \quad R^2=0.78 \quad \dots (35)$$

$$\epsilon_A = 0.8e^{0.16n} \quad R^2=0.79 \quad \dots (36)$$

$$\gamma_A = 0.4e^{0.16n} \quad R^2=0.79 \quad \dots (37)$$

The comparisons of amplitude anisotropy and amplitude ratios of P and S waves depending on the curing conditions were shown in Fig. 11.

In this figure, amplitude anisotropy and amplitude ratio of P waves in water cure were obtained higher than those in air cure. This situation was mostly

observed in low strength concretes. On the other hand, it was not clearly seen the difference in the amplitude anisotropy and ratio values of S waves in water or air curing. This was because S waves less affected by the pore saturation in concrete.

#### 4 Conclusion

It has seen that anisotropy in the reinforced concrete can be nondestructively determined by signal analysis of ultrasonic waves in this study. According to this study, S wave amplitudes have generally obtained higher than P wave amplitudes that determined from the same surface. However, amplitude values may not be alone meaningful in terms of interpretation of anisotropy in concrete. Therefore, the presence and degree of anisotropy in concretes with different strengths can be revealed by calculating the amplitude ratio and amplitude anisotropy.

While amplitude ratio and anisotropies of P and S waves have increased with decreasing of concrete strength, they have increased with increasing of porosity of concrete. In addition, amplitude anisotropy and amplitude ratio of P wave in water saturated samples have generally higher than that of P wave in air saturated samples. The amplitude anisotropy and amplitude ratio of the S wave have closer to each other in water and air cured samples. Because S wave has not affected by saturation type of samples pores. Also, curing conditions, porosity and concrete strength have an effect on amplitude anisotropy and ratio.

According to this study, new equations have determined between P and S wave amplitude anisotropy and reinforcement diameter for low, medium and high strength reinforced concrete depending on curing conditions. As can be seen from these equations, it should be thought that the reason for the increase in anisotropy due to the increase in the diameter of the reinforcement has not only the effect of the reinforcement but also the strength effect.

P or S wave amplitude anisotropies or amplitude ratios can be estimated from UCS or porosity of the concrete by using new equations developed in this study. However, the limit ranges of these equations cannot be ignored for anisotropy estimation from UCS and porosity values (UCS: 5-62 MPa, n: 2-12%).

#### Acknowledgement

The author thanks the anonymous reviewers, Assoc. Prof. Dr. Osman UYANIK and Dr. Ziya

ÖNCÜ for their support, positive contributions and valuable suggestions.

#### References

- 1 Popovics J S, & Rose J L, *IEEE Trans Ultrason Ferroelectr Freq Control*, 41 (1994) 140.
- 2 Shah A A, Alsayed S H, Abbas H, & Al-Salloum Y A, *Cons Build Mater*, 29 (2012) 42.
- 3 Karaiskos G, Tsangouri E, Aggelis D G, Van K, Belie N D, & Hemelrijck D V, *Damage Detection and Healing Performance Monitoring using Embedded Piezoelectric Transducers in Large- Scale Concrete Structures*, 19<sup>th</sup> World Conference on Non-Dest. Testing, ISBN: 978-3-940283-78-8 (2016) 1.
- 4 Shokouhi P, Zoega A, & Wiggenhauser H, *Adv Civ Eng Mater*, 740189 (2010) 9.
- 5 Benedetto A, Tosti F, Ciampoli L B, & Damico F, *Signal Process*, 132 (2017) 201.
- 6 Prassianakis I N, & Prassianakis N I, *Theor Appl Fract Mech*, 42 (2004) 191.
- 7 Schubert F, *Ultrasonics*, 42 (2004) 221.
- 8 Payan C, Garnier V, & Moysan J, *Adv Civil Eng*, 238472 (2010) 8.
- 9 Malhotra V M & Carino N J, *Handbook on nondestructive testing of concrete*, (CRC Press, New York), ISBN:9780849314858(2004) 384.
- 10 Gül R, Demirboga R, & Güvercin T, *Indian J Eng Mater Sci*, 13 (2006) 18.
- 11 Ju W J, Weng L S, & Liu Y, *ACI Mater J*, 103 (2006) 177.
- 12 Yazicioglu S, Caliskan S, & Türk K, *Indian J Eng Mater Sci*, 13 (2006) 25.
- 13 Shah A A, & Ribakov Y, *Materials and Design*, 32 (2011) 4122.
- 14 Uyanık O, Kaptan K, Gülay F G, & Tezcan S, *Yapı Dünyası*, 184 (2011) 55.
- 15 Uyanık O, Şenli G & Çathoğlu B, *SDU Int Tech Sci*, 5 (2013) 156.
- 16 Sabbağ N, & Uyanık O, *Online J Sci Technol*, 6 (2016) 4.
- 17 Sabbağ N, & Uyanık O, *J Appl Sci Eng*, 18 (2018) 1181.
- 18 Kassab M A, & Weller A, *Egypt J Pet*, (2019). DOI:10.1016/j.ejpe.2019.03.003.
- 19 Uyanık O, Sabbağ N, Uyanık N A, & Öncü Z, *Bull Eng Geol Environ*, 78 (2019) 6003.
- 20 Karahan Ş, Büyüksaraç A, & Işık E, *Iran J Sci Technol - Trans Civ Eng*, 44 (2020) 91.
- 21 Işık E, Büyüksaraç A, Aşar E, Kuluöztürk MF & Günay M, *Mater Constr*, 70 (2020) 338.
- 22 Ekin N, & Uyanık O, *Iran J Sci Technol - Trans Civ Eng*, (2021) DOI: 10.1007/s40996-020-00513-7 (in press).
- 23 Gu H, Song G, Dhonde H, Mo Y L, & Yan S, *Smart Mater Struct*, 15 (2006) 1837.
- 24 Oziçer S, & Uyanık O, *Int J Eng Sci Technol*, 9 (2017) 1.
- 25 Schubert F, & Marklein R, *Numerical Computation of Ultrasonic Wave Propagation in Concrete using the Elastodynamic Finite Integration Technique (EFIT)*, IEEE Ultras Symp, ISBN:0-7803-7582-3(2002)799.
- 26 Sabbağ N, & Uyanık O, *Pamukkale Uni J Eng Sci*, 26(3) (2020) 572.
- 27 Kolkoori S R, Rahman M U, Chinta P K, Ktreutzbruck M, Rethmeier M, & Prager J, *Ultrasonics*, 53 (2013) 396.
- 28 Niederleithinger E, Wolf J, Mielentz F, Wiggenhauser H, & Pirskawetz S, *Sensors*, 15 (2015) 9756.

- 29 Popovics S, *Materials Evaluation*, (2001) 123.
- 30 Prassianakis I N, & Giokas P, *Mag Concr Res*, 55 (2003) 171.
- 31 Prassianakis I N, *The characterization of an old concrete using destructive and the ultrasonic non-destructive testing methods*, in: Proceedings of the 8<sup>th</sup> European Conference on NDT, Barcelona Spain, ISBN: 84-699-8573- 6(2002) 17.
- 32 Bessinger BA, Suárez-Rivera R, Nihei KT, Hilbert LB, Myer LR & Cook NGW, *Advances in Anisotropy, Society of Exploration Geophysicists*, (2001) 333.
- 33 Sabbağ N, & Uyanık O, *Pamukkale Uni J Eng Sci*, 24(6) (2018) 1230.
- 34 Nogueira C L, & William K J, *ACI Mater J*, 98 (2001) 265.
- 35 Uyanık O, *UCTEA Chamber of Geophysical Engineers Geophysical Bulletin*, (2012) 25.
- 36 Sabbağ N, & Uyanık O, *J Appl Geophys*, 141 (2017) 13.
- 37 Rao MVMS, & Lakshmi KJP, *Current science*, 85 (2003) 1221.
- 38 Uyanık O, & Tezcan S, *UCTEA Chamber of Geophysical Engineers Geophysical Bulletin*, (2012) 41.
- 39 Uyanık O, & Çathioğlu B, *UCTEA Chamber of Geophysical Engineers Geophysical Bulletin*, 17 (2015) 3.
- 40 Shah A A, & Ribakov Y, *Materials and Design*, 30 (2009) 4095.
- 41 Pahlavan L, Zhang F, Blacquièrè G, Yang Y, & Hordijk D, *Constr Build Mater*, 167 (2018) 899.
- 42 Popovics J S, Song W J, Ghandehari M, Subramaniam K V, Achenbach J D, & Shah S P, *ACI Struct J*, 97 (2000) 127.
- 43 Liu P L, Lee K H, Wu T T, & Kuo MK, *NDT E Int*, 34 (2001) 219.
- 44 Masserey B & Mazza E, *J Acoust Soc Am*, 118 (2005) 3585.
- 45 Zerwer A, Polak M A, & Santamarina J C, *J Environ Eng Geophys*, 10 (2005) 295.
- 46 Shin S W, Zhu J, Min J, & Popovics J S, *ACI Mater J*, 105 (2008) 510.
- 47 Aggelis D G, Shiotani T, & Polyzos D, *Cem Concr Compos*, 31 (2009) 77.
- 48 Kee S H, & Zhu J, *ACI Mater J*, 111(2014) 35.
- 49 Kupperman D S, & Kejmman K J, *IEEE Trans Sonics Ultras*, 27 (1980) 7.
- 50 Sayers C M, Van Munster J G, & King M S, *Int J Rock Mech Min Sci*, 27 (1990) 429.
- 51 Cohen L, *Time-Frequency Distributions - A Review*, Proc IEEE, 77 (1989) 941.
- 52 Ayu H D, & Sarwanto S, *Analysis of seismic signal in order to determine subsurface Characteristics*, Annual Conference of Science and Technology Journal of Physics: Conference Series IOP Publishing, 1375 (2019) 012079.
- 53 Cohen L, *Time Frequency Analysis*, Prentice-Hall, New Jersey, 5(2) (1995) 292.
- 54 Zdiri M, Abriak N, Ouedzou M B, & Neji J, *Int J Concr Struct Mater*, 4 (2010) 45.
- 55 Hemsing D, & Schmitt D, *Laboratory determination of elastic anisotropy of shales from Alberta*, SEG 76<sup>th</sup> Annual Meeting, New Orleans, (2006) 229.
- 56 Koesoemadinata A P, & Mc Mechan G A, *J Appl Geophys*, 56 (2004) 165.
- 57 Naik T R, Malhotra V M, & Popovics J S, *Handbook on Nondestructive Testing of Concrete*, Ed. Malhotra V M and Carino N J (CRC Press, New York), ISBN-13: 978-0849314858 (2004) 19.
- 58 Lorenzi A, Tisbierek F T, & Silva Filho LCP, *Ultrasonic Pulse Velocity Analysis in Concrete Specimens*, IV Conferencia Panamericana de END Buenos Aires, Octubre (2007) 13.
- 59 Torrijos M C, Barragan B E, & Zerbino R L, *Constr Build Mater*, 22 (2008) 1780.
- 60 Benaicha M, Jalbaud O, Roguiez X, Alaoui A H, & Burtschell Y, *Alex Eng J*, 54 (2015) 1181.
- 61 Warnemuende K, *Amplitude Modulated Acoustoultrasonic Non-Destructive Testing: Damage Evaluation in Concrete*, PhD. Thesis, Wayne State University, 2006.
- 62 Daponte P, Maceri F, & Olivito RS, *IEEE Trans Instrum Meas*, 4 (1995) 1003.
- 63 Thomsen L, *Geophysics*, 51 (1986) 1954.